BABAR-CONF-02/25
SLAC-PUB-9308
hep-ex/0207074
July 2002

$b \to s\gamma$ using a Sum of Exclusive Modes

The *BABAR* Collaboration

July 24, 2002

Abstract

This paper describes preliminary results on the inclusive process $b \to s\gamma$ obtained from 20.7 fb^{-1} of data recorded with the *BABAR* detector during 1999-2000. Signal event yields are found from a combination of twelve exclusive decay channels after subtracting continuum and $B\overline{B}$ backgrounds. Cross–feed from incorrectly reconstructed $b \to s\gamma$ events is also removed. Branching fractions in bins of hadronic mass are calculated using corrected Monte Carlo signal efficiencies; this is equivalent to measuring the gamma energy spectrum. We measure the first moment of the gamma energy spectrum constraining the HQET parameter $\overline{\Lambda} = 0.37 \pm 0.09\ (stat) \pm 0.07\ (syst) \pm 0.10\ (model)$ GeV/c^2. A fit to the hadronic mass spectrum gives $\mathcal{B}(b \to s\gamma) = (4.3 \pm 0.5\ (stat) \pm 0.8\ (syst) \pm 1.3\ (model)) \cdot 10^{-4}$ for the inclusive branching fraction. We also constrain the HQET parameter λ_1.

Contributed to the 31^{st} International Conference on High Energy Physics,
7/24—7/31/2002, Amsterdam, The Netherlands

Stanford Linear Accelerator Center, Stanford University, Stanford, CA 94309

Work supported in part by Department of Energy contract DE-AC03-76SF00515.

The *BABAR* Collaboration,

B. Aubert, D. Boutigny, J.-M. Gaillard, A. Hicheur, Y. Karyotakis, J. P. Lees, P. Robbe, V. Tisserand, A. Zghiche

Laboratoire de Physique des Particules, F-74941 Annecy-le-Vieux, France

A. Palano, A. Pompili

Università di Bari, Dipartimento di Fisica and INFN, I-70126 Bari, Italy

J. C. Chen, N. D. Qi, G. Rong, P. Wang, Y. S. Zhu

Institute of High Energy Physics, Beijing 100039, China

G. Eigen, I. Ofte, B. Stugu

University of Bergen, Inst. of Physics, N-5007 Bergen, Norway

G. S. Abrams, A. W. Borgland, A. B. Breon, D. N. Brown, J. Button-Shafer, R. N. Cahn, E. Charles, M. S. Gill, A. V. Gritsan, Y. Groysman, R. G. Jacobsen, R. W. Kadel, J. Kadyk, L. T. Kerth, Yu. G. Kolomensky, J. F. Kral, C. LeClerc, M. E. Levi, G. Lynch, L. M. Mir, P. J. Oddone, T. J. Orimoto, M. Pripstein, N. A. Roe, A. Romosan, M. T. Ronan, V. G. Shelkov, A. V. Telnov, W. A. Wenzel

Lawrence Berkeley National Laboratory and University of California, Berkeley, CA 94720, USA

T. J. Harrison, C. M. Hawkes, D. J. Knowles, S. W. O'Neale, R. C. Penny, A. T. Watson, N. K. Watson

University of Birmingham, Birmingham, B15 2TT, United Kingdom

T. Deppermann, K. Goetzen, H. Koch, B. Lewandowski, K. Peters, H. Schmuecker, M. Steinke

Ruhr Universität Bochum, Institut für Experimentalphysik 1, D-44780 Bochum, Germany

N. R. Barlow, W. Bhimji, J. T. Boyd, N. Chevalier, P. J. Clark, W. N. Cottingham, C. Mackay, F. F. Wilson

University of Bristol, Bristol BS8 1TL, United Kingdom

K. Abe, C. Hearty, T. S. Mattison, J. A. McKenna, D. Thiessen

University of British Columbia, Vancouver, BC, Canada V6T 1Z1

S. Jolly, A. K. McKemey

Brunel University, Uxbridge, Middlesex UB8 3PH, United Kingdom

V. E. Blinov, A. D. Bukin, A. R. Buzykaev, V. B. Golubev, V. N. Ivanchenko, A. A. Korol, E. A. Kravchenko, A. P. Onuchin, S. I. Serednyakov, Yu. I. Skovpen, A. N. Yushkov

Budker Institute of Nuclear Physics, Novosibirsk 630090, Russia

D. Best, M. Chao, D. Kirkby, A. J. Lankford, M. Mandelkern, S. McMahon, D. P. Stoker

University of California at Irvine, Irvine, CA 92697, USA

C. Buchanan, S. Chun

University of California at Los Angeles, Los Angeles, CA 90024, USA

H. K. Hadavand, E. J. Hill, D. B. MacFarlane, H. Paar, S. Prell, Sh. Rahatlou, G. Raven, U. Schwanke, V. Sharma

University of California at San Diego, La Jolla, CA 92093, USA

J. W. Berryhill, C. Campagnari, B. Dahmes, P. A. Hart, N. Kuznetsova, S. L. Levy, O. Long, A. Lu, M. A. Mazur, J. D. Richman, W. Verkerke

University of California at Santa Barbara, Santa Barbara, CA 93106, USA

J. Beringer, A. M. Eisner, M. Grothe, C. A. Heusch, W. S. Lockman, T. Pulliam, T. Schalk, R. E. Schmitz, B. A. Schumm, A. Seiden, M. Turri, W. Walkowiak, D. C. Williams, M. G. Wilson

University of California at Santa Cruz, Institute for Particle Physics, Santa Cruz, CA 95064, USA

E. Chen, G. P. Dubois-Felsmann, A. Dvoretskii, D. G. Hitlin, F. C. Porter, A. Ryd, A. Samuel, S. Yang

California Institute of Technology, Pasadena, CA 91125, USA

S. Jayatilleke, G. Mancinelli, B. T. Meadows, M. D. Sokoloff

University of Cincinnati, Cincinnati, OH 45221, USA

T. Barillari, P. Bloom, W. T. Ford, U. Nauenberg, A. Olivas, P. Rankin, J. Roy, J. G. Smith, W. C. van Hoek, L. Zhang

University of Colorado, Boulder, CO 80309, USA

J. L. Harton, T. Hu, M. Krishnamurthy, A. Soffer, W. H. Toki, R. J. Wilson, J. Zhang

Colorado State University, Fort Collins, CO 80523, USA

D. Altenburg, T. Brandt, J. Brose, T. Colberg, M. Dickopp, R. S. Dubitzky, A. Hauke, E. Maly, R. Müller-Pfefferkorn, S. Otto, K. R. Schubert, R. Schwierz, B. Spaan, L. Wilden

Technische Universität Dresden, Institut für Kern- und Teilchenphysik, D-01062 Dresden, Germany

D. Bernard, G. R. Bonneaud, F. Brochard, J. Cohen-Tanugi, S. Ferrag, S. T'Jampens, Ch. Thiebaux, G. Vasileiadis, M. Verderi

Ecole Polytechnique, LLR, F-91128 Palaiseau, France

A. Anjomshoaa, R. Bernet, A. Khan, D. Lavin, F. Muheim, S. Playfer, J. E. Swain, J. Tinslay

University of Edinburgh, Edinburgh EH9 3JZ, United Kingdom

M. Falbo

Elon University, Elon University, NC 27244-2010, USA

C. Borean, C. Bozzi, L. Piemontese, A. Sarti

Università di Ferrara, Dipartimento di Fisica and INFN, I-44100 Ferrara, Italy

E. Treadwell

Florida A&M University, Tallahassee, FL 32307, USA

F. Anulli,[1] R. Baldini-Ferroli, A. Calcaterra, R. de Sangro, D. Falciai, G. Finocchiaro, P. Patteri, I. M. Peruzzi,[1] M. Piccolo, A. Zallo

Laboratori Nazionali di Frascati dell'INFN, I-00044 Frascati, Italy

S. Bagnasco, A. Buzzo, R. Contri, G. Crosetti, M. Lo Vetere, M. Macri, M. R. Monge, S. Passaggio, F. C. Pastore, C. Patrignani, E. Robutti, A. Santroni, S. Tosi

Università di Genova, Dipartimento di Fisica and INFN, I-16146 Genova, Italy

[1]Also with Università di Perugia, I-06100 Perugia, Italy

S. Bailey, M. Morii

Harvard University, Cambridge, MA 02138, USA

R. Bartoldus, G. J. Grenier, U. Mallik

University of Iowa, Iowa City, IA 52242, USA

J. Cochran, H. B. Crawley, J. Lamsa, W. T. Meyer, E. I. Rosenberg, J. Yi

Iowa State University, Ames, IA 50011-3160, USA

M. Davier, G. Grosdidier, A. Höcker, H. M. Lacker, S. Laplace, F. Le Diberder, V. Lepeltier, A. M. Lutz, T. C. Petersen, S. Plaszczynski, M. H. Schune, L. Tantot, S. Trincaz-Duvoid, G. Wormser

Laboratoire de l'Accélérateur Linéaire, F-91898 Orsay, France

R. M. Bionta, V. Brigljević , D. J. Lange, K. van Bibber, D. M. Wright

Lawrence Livermore National Laboratory, Livermore, CA 94550, USA

A. J. Bevan, J. R. Fry, E. Gabathuler, R. Gamet, M. George, M. Kay, D. J. Payne, R. J. Sloane, C. Touramanis

University of Liverpool, Liverpool L69 3BX, United Kingdom

M. L. Aspinwall, D. A. Bowerman, P. D. Dauncey, U. Egede, I. Eschrich, G. W. Morton, J. A. Nash, P. Sanders, D. Smith, G. P. Taylor

University of London, Imperial College, London, SW7 2BW, United Kingdom

J. J. Back, G. Bellodi, P. Dixon, P. F. Harrison, R. J. L. Potter, H. W. Shorthouse, P. Strother, P. B. Vidal

Queen Mary, University of London, E1 4NS, United Kingdom

G. Cowan, H. U. Flaecher, S. George, M. G. Green, A. Kurup, C. E. Marker, T. R. McMahon, S. Ricciardi, F. Salvatore, G. Vaitsas, M. A. Winter

University of London, Royal Holloway and Bedford New College, Egham, Surrey TW20 0EX, United Kingdom

D. Brown, C. L. Davis

University of Louisville, Louisville, KY 40292, USA

J. Allison, R. J. Barlow, A. C. Forti, F. Jackson, G. D. Lafferty, A. J. Lyon, N. Savvas, J. H. Weatherall, J. C. Williams

University of Manchester, Manchester M13 9PL, United Kingdom

A. Farbin, A. Jawahery, V. Lillard, D. A. Roberts, J. R. Schieck

University of Maryland, College Park, MD 20742, USA

G. Blaylock, C. Dallapiccola, K. T. Flood, S. S. Hertzbach, R. Kofler, V. B. Koptchev, T. B. Moore, H. Staengle, S. Willocq

University of Massachusetts, Amherst, MA 01003, USA

B. Brau, R. Cowan, G. Sciolla, F. Taylor, R. K. Yamamoto

Massachusetts Institute of Technology, Laboratory for Nuclear Science, Cambridge, MA 02139, USA

M. Milek, P. M. Patel

McGill University, Montréal, QC, Canada H3A 2T8

F. Palombo

Università di Milano, Dipartimento di Fisica and INFN, I-20133 Milano, Italy

J. M. Bauer, L. Cremaldi, V. Eschenburg, R. Kroeger, J. Reidy, D. A. Sanders, D. J. Summers

University of Mississippi, University, MS 38677, USA

C. Hast, P. Taras

Université de Montréal, Laboratoire René J. A. Lévesque, Montréal, QC, Canada H3C 3J7

H. Nicholson

Mount Holyoke College, South Hadley, MA 01075, USA

C. Cartaro, N. Cavallo, G. De Nardo, F. Fabozzi, C. Gatto, L. Lista, P. Paolucci, D. Piccolo, C. Sciacca

Università di Napoli Federico II, Dipartimento di Scienze Fisiche and INFN, I-80126, Napoli, Italy

J. M. LoSecco

University of Notre Dame, Notre Dame, IN 46556, USA

J. R. G. Alsmiller, T. A. Gabriel

Oak Ridge National Laboratory, Oak Ridge, TN 37831, USA

J. Brau, R. Frey, M. Iwasaki, C. T. Potter, N. B. Sinev, D. Strom, E. Torrence

University of Oregon, Eugene, OR 97403, USA

F. Colecchia, A. Dorigo, F. Galeazzi, M. Margoni, M. Morandin, M. Posocco, M. Rotondo, F. Simonetto, R. Stroili, C. Voci

Università di Padova, Dipartimento di Fisica and INFN, I-35131 Padova, Italy

M. Benayoun, H. Briand, J. Chauveau, P. David, Ch. de la Vaissière, L. Del Buono, O. Hamon, Ph. Leruste, J. Ocariz, M. Pivk, L. Roos, J. Stark

Universités Paris VI et VII, Lab de Physique Nucléaire H. E., F-75252 Paris, France

P. F. Manfredi, V. Re, V. Speziali

Università di Pavia, Dipartimento di Elettronica and INFN, I-27100 Pavia, Italy

L. Gladney, Q. H. Guo, J. Panetta

University of Pennsylvania, Philadelphia, PA 19104, USA

C. Angelini, G. Batignani, S. Bettarini, M. Bondioli, F. Bucci, G. Calderini, E. Campagna, M. Carpinelli, F. Forti, M. A. Giorgi, A. Lusiani, G. Marchiori, F. Martinez-Vidal, M. Morganti, N. Neri, E. Paoloni, M. Rama, G. Rizzo, F. Sandrelli, G. Triggiani, J. Walsh

Università di Pisa, Scuola Normale Superiore and INFN, I-56010 Pisa, Italy

M. Haire, D. Judd, K. Paick, L. Turnbull, D. E. Wagoner

Prairie View A&M University, Prairie View, TX 77446, USA

J. Albert, G. Cavoto,[2] N. Danielson, P. Elmer, C. Lu, V. Miftakov, J. Olsen, S. F. Schaffner, A. J. S. Smith, A. Tumanov, E. W. Varnes

Princeton University, Princeton, NJ 08544, USA

[2]Also with Università di Roma La Sapienza, Roma, Italy

F. Bellini, D. del Re, R. Faccini,[3] F. Ferrarotto, F. Ferroni, E. Leonardi, M. A. Mazzoni, S. Morganti, G. Piredda, F. Safai Tehrani, M. Serra, C. Voena

Università di Roma La Sapienza, Dipartimento di Fisica and INFN, I-00185 Roma, Italy

S. Christ, G. Wagner, R. Waldi

Universität Rostock, D-18051 Rostock, Germany

T. Adye, N. De Groot, B. Franek, N. I. Geddes, G. P. Gopal, S. M. Xella

Rutherford Appleton Laboratory, Chilton, Didcot, Oxon, OX11 0QX, United Kingdom

R. Aleksan, S. Emery, A. Gaidot, P.-F. Giraud, G. Hamel de Monchenault, W. Kozanecki, M. Langer, G. W. London, B. Mayer, G. Schott, B. Serfass, G. Vasseur, Ch. Yeche, M. Zito

DAPNIA, Commissariat à l'Energie Atomique/Saclay, F-91191 Gif-sur-Yvette, France

M. V. Purohit, A. W. Weidemann, F. X. Yumiceva

University of South Carolina, Columbia, SC 29208, USA

I. Adam, D. Aston, N. Berger, A. M. Boyarski, M. R. Convery, D. P. Coupal, D. Dong, J. Dorfan, W. Dunwoodie, R. C. Field, T. Glanzman, S. J. Gowdy, E. Grauges , T. Haas, T. Hadig, V. Halyo, T. Himel, T. Hryn'ova, M. E. Huffer, W. R. Innes, C. P. Jessop, M. H. Kelsey, P. Kim, M. L. Kocian, U. Langenegger, D. W. G. S. Leith, S. Luitz, V. Luth, H. L. Lynch, H. Marsiske, S. Menke, R. Messner, D. R. Muller, C. P. O'Grady, V. E. Ozcan, A. Perazzo, M. Perl, S. Petrak, H. Quinn, B. N. Ratcliff, S. H. Robertson, A. Roodman, A. A. Salnikov, T. Schietinger, R. H. Schindler, J. Schwiening, G. Simi, A. Snyder, A. Soha, S. M. Spanier, J. Stelzer, D. Su, M. K. Sullivan, H. A. Tanaka, J. Va'vra, S. R. Wagner, M. Weaver, A. J. R. Weinstein, W. J. Wisniewski, D. H. Wright, C. C. Young

Stanford Linear Accelerator Center, Stanford, CA 94309, USA

P. R. Burchat, C. H. Cheng, T. I. Meyer, C. Roat

Stanford University, Stanford, CA 94305-4060, USA

R. Henderson

TRIUMF, Vancouver, BC, Canada V6T 2A3

W. Bugg, H. Cohn

University of Tennessee, Knoxville, TN 37996, USA

J. M. Izen, I. Kitayama, X. C. Lou

University of Texas at Dallas, Richardson, TX 75083, USA

F. Bianchi, M. Bona, D. Gamba

Università di Torino, Dipartimento di Fisica Sperimentale and INFN, I-10125 Torino, Italy

L. Bosisio, G. Della Ricca, S. Dittongo, L. Lanceri, P. Poropat, L. Vitale, G. Vuagnin

Università di Trieste, Dipartimento di Fisica and INFN, I-34127 Trieste, Italy

R. S. Panvini

Vanderbilt University, Nashville, TN 37235, USA

[3]Also with University of California at San Diego, La Jolla, CA 92093, USA

S. W. Banerjee, C. M. Brown, D. Fortin, P. D. Jackson, R. Kowalewski, J. M. Roney

University of Victoria, Victoria, BC, Canada V8W 3P6

H. R. Band, S. Dasu, M. Datta, A. M. Eichenbaum, H. Hu, J. R. Johnson, R. Liu, F. Di Lodovico, A. Mohapatra, Y. Pan, R. Prepost, I. J. Scott, S. J. Sekula, J. H. von Wimmersperg-Toeller, J. Wu, S. L. Wu, Z. Yu

University of Wisconsin, Madison, WI 53706, USA

H. Neal

Yale University, New Haven, CT 06511, USA

1 Introduction

The $b \to s\gamma$ transition proceeds by an effective flavor-changing neutral current. The Standard Model prediction, in which the t penguin loop gives the largest contribution, has been calculated to next–to–leading order [1]. Measurements of the inclusive branching fraction have been used to constrain new physics contributions to the decay amplitude [2].

Since $b \to s\gamma$ is a two–body decay process, the photon energy, E_γ, in the B rest frame, is related to the recoil hadronic mass, M_{Had}, by:

$$E_\gamma = \frac{M_B^2 - {M_{Had}}^2}{2M_B}. \tag{1}$$

In our analysis we fully reconstruct twelve exclusive $b \to s\gamma$ decays, and use the hadronic mass spectrum to measure the photon energy spectrum in the B rest frame. Note that in a fully inclusive analysis [3], where only the photon is measured, the gamma energy is smeared by the resolution of the calorimeter and by the motion of the B meson in the $\Upsilon(4S)$ rest frame. With our semi-exclusive approach, the gamma energy resolution depends only on the M_{Had} resolution, which is a few MeV/c^2.

We fit the M_{Had} spectrum with the model proposed by Kagan and Neubert [4], which predicts the shape of the gamma energy spectrum using heavy quark effective theory (HQET). There are two main parameters, an effective b quark mass, m_b, and λ_1, which is related to the kinetic energy of the b quark in the B meson. The model introduces the known $K^*\gamma$ contribution [5] using local quark-hadron duality to convert the portion of the spectrum below a cutoff mass into a $K^*(892)$ Breit-Wigner shape. The cutoff mass is a free parameter in the model, but is expected to be between 1.0 and 1.2 GeV/c^2. Above this cutoff the inclusive model does not explicitly include any higher resonances.

We find a correlated band of allowed values for the parameters m_b and λ_1, and a cutoff mass of about 1.11 GeV/c^2. By measuring the first moment of the photon energy spectrum we constrain the HQET parameter $\bar{\Lambda}$ and hence m_b. A fit to the M_{Had} spectrum with this constraint applied to m_b gives the inclusive branching fraction and a range of values for λ_1. There is currently much interest in the HQET parameters, since they are needed to extract V_{ub} and V_{cb} from semileptonic B decays [6].

2 The *BABAR* detector and dataset

This paper describes preliminary results obtained from 20.7 fb^{-1} of data recorded with the *BABAR* detector at the PEP-II asymmetric e^+e^- storage ring during 1999-2000. The data correspond to a total of $(22.74 \pm 0.36) \cdot 10^6$ $B\overline{B}$ pairs collected on the $\Upsilon(4S)$ resonance.

The *BABAR* detector is described in detail elsewhere [7]. We briefly summarize the detector systems most relevant to the current paper. The *BABAR* detector contains a five–layer silicon vertex tracker (SVT) and a forty–layer drift chamber (DCH) situated in a 1.5 T solenoidal magnetic field. These devices detect charged particles and measure their momentum and ionization energy loss (dE/dx). The transverse momentum resolution is $\sigma_{p_t}/p_t = (0.13 \pm 0.01)\% \cdot p_t + (0.45 \pm 0.03)\%$, with p_t in GeV/c. Photons are detected in a CsI(Tl) crystal electromagnetic calorimeter (EMC). The EMC detects photons with energies as low as 20 MeV. The nominal EMC resolution for photons and electrons is $\sigma_E/E = 2.3\%/E^{1/4} \oplus 1.9\%$, with E in GeV. The charged particle identification (PID) combines dE/dx measurements in the SVT and DCH with particle velocity measurements,

obtained with an internally reflecting ring-imaging Cherenkov detector (DIRC) of quartz bars surrounding the DCH.

The interactions of particles traversing the detector are simulated using GEANT4 [8]. Variations in detector conditions and beam-induced backgrounds are taken into account in these simulations. Signal and generic background samples are used to study the effect of the event selection criteria and to estimate the backgrounds. The generic background simulations consist of $e^+e^- \to q\overline{q}$ ($q = u, d, s, c$) and $B\overline{B}$ events, where the $b \to s\gamma$ signal events have been removed.

3 Event Selection

We reconstruct 12 final states[1] formed from a high–energy photon, a charged or neutral kaon, and 1-3 pions, one of which can be neutral:

$$K^+\pi^-,\ K_S\pi^0,\ K^+\pi^-\pi^0,\ K_S\pi^+\pi^-,\ K^+\pi^-\pi^+\pi^-,\ K_S\pi^+\pi^-\pi^0$$

$$K^+\pi^0,\ K_S\pi^+,\ K^+\pi^-\pi^+,\ K_S\pi^+\pi^0,\ K^+\pi^-\pi^+\pi^0,\ K_S\pi^+\pi^-\pi^+$$

These make up about 50% of the total $b \to s\gamma$ rate for $M_{Had} < 2.4$ GeV/c^2.

We select events with at least one photon with an energy $1.5 < E^*_\gamma < 3.5$ GeV in the e^+e^- centre-of-mass (CM) frame. If the photon can be combined with another photon with energy > 50 MeV (250 MeV) to make a π^0 (η) with a mass between 115 MeV/c^2 (508 MeV/c^2) and 155 MeV/c^2 (588 MeV/c^2), it is vetoed.

In the hadronic system, a π^0 is made from two photons, with a minimum photon energy of 30 MeV, and a minimum π^0 energy of 200 MeV. Well reconstructed tracks are used for charged pions, but charged kaons must satisfy additional kaon identification criteria. Candidates for $K_S \to \pi^+\pi^-$ decays are selected by requiring a mass between 489 and 507 MeV/c^2, and a decay length > 2 mm. These kaon selections reduce any $b \to d\gamma$ background contributions to a negligible level.

The mass of the hadronic system is restricted to:

$$0.6 < M_{Had} < 2.4 \text{ GeV}/c^2$$

where the upper limit corresponds to a requirement on $E_\gamma > 2.094$ GeV. Most of the background is accounted for by events in which the photon comes from initial state radiation (ISR) or from π^0/η decays that survive the veto. We suppress these by requiring $\cos\theta_{T^*} < 0.7$, where $\cos\theta_{T^*}$ is the angle in the CM system between the high–energy photon candidate and the thrust axis of the rest of the event calculated after removing the B candidate. Further suppression is achieved by combining several event shape variables in a Fisher discriminant. The variables include the ratio of the second and zeroth Fox Wolfram moments [9] computed in the CM and in the photon recoil system, the CM direction of the B candidate, and energy flow in a 20° cone along the photon direction and in a 40° cone opposite the photon.

The hadronic system is combined with a high–energy photon, and accepted as a B candidate if the energy in the CM system, E^*_B, is within 150 MeV of the CM beam energy, E^*_{beam}, :

$$|\Delta E| = |E^*_B - E^*_{beam}| < 150 \text{ MeV} \tag{2}$$

and the beam-energy substituted mass $m_{\rm ES}$:

$$m_{\rm ES} = \sqrt{E^{*2}_{beam} - p^{*2}_B} > 5.21 \text{ GeV}/c^2 \tag{3}$$

[1] Charge conjugate modes are assumed throughout this paper.

where p_B^* is the B momentum in the CM frame.

If there is more than one B candidate left in an event, we choose the candidate with the minimum $|\Delta E|$. Then, we rescale the measured photon energy to give $\Delta E = 0$ GeV, and recalculate $m_{\rm ES}$. This corrects for energy leakage and improves the $m_{\rm ES}$ resolution, particularly for candidates without a π^0.

4 Background Subtraction

The background is mainly from continuum, although $B\overline{B}$ backgrounds become significant at high M_{Had} values. The continuum background $m_{\rm ES}$ distribution can be fit by an ARGUS [10] function. When divided into bins in M_{Had}, the generic continuum Monte Carlo samples show a slight dependence of the shape parameter of the ARGUS function on M_{Had}, which we take into account in our fits.

The $B\overline{B}$ background is mainly composed of final states with high multiplicity and high hadronic mass, where the photon is the daughter of a π^0 or η that decayed asymmetrically. We fit the generic $B\overline{B}$ Monte Carlo samples with an ARGUS function for the non-peaking background and a Crystal Ball function [11] for the peaking background, such as $B \to D^{(*)}\rho^-$ where only a low–energy photon is missing. The shape parameters of the ARGUS functions for the continuum and non-peaking $B\overline{B}$ backgrounds are sufficiently similar that it is possible to use a combined ARGUS function to describe the sum of the two backgrounds.

Figure 1 shows the continuum and non-peaking $B\overline{B}$ backgrounds for $m_{\rm ES} > 5.21$ GeV/c^2, in bins of hadronic mass. The level of $B\overline{B}$ background is only significant for $M_{Had} > 1.8$ GeV/c^2.

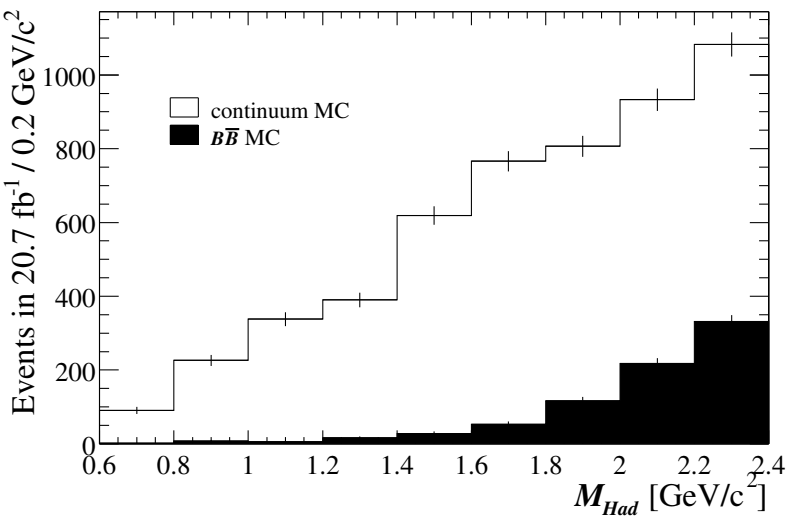

Figure 1: Expected continuum and $B\overline{B}$ background events in 20.7 fb^{-1} from Monte Carlo (MC) simulation as a function of the hadronic mass.

We treat $b \to s\gamma$ events as "cross-feed" background when they are reconstructed with the correct photon, but with the wrong hadronic system, since this gives an incorrect measurement of M_{Had}. Cross-feed events come from three sources, which are, in decreasing order of importance:

- Final states that are not considered in the analysis, e.g. K_L, $\geq 2\pi^0$, ≥ 5–body hadronic final states, and events with $M_{Had} > 2.4$ GeV/c^2;

- Final states which are considered, but in which one of the final state particles is not detected; and
- Multiple candidate events where the wrong candidate is chosen.

The cross-feed $m_{\rm ES}$ distribution is fit with an ARGUS function plus the Crystal Ball function to allow for a possible peaking contribution. The cross-feed ARGUS function rises towards the signal region. Note that the level of cross-feed background is proportional to the inclusive branching fraction. The peaking component of the cross-feed background contributes just a few events.

Fits to the $m_{\rm ES}$ distributions of data events are performed in each of the nine M_{Had} bins using a Crystal Ball function for the contributions that peak in the signal region and two ARGUS functions for the non-peaking backgrounds. The plots of the fits to the eight M_{Had} bins from 0.8 to 2.4 GeV/c^2 can be seen in Figure 2.

Table 1 lists the peaking yields for the sum of all final states in data, $B\overline{B}$ Monte Carlo and cross–feed, normalized to our measured inclusive branching fraction.

M_{Had} [GeV/c^2]	data	$B\overline{B}$	cross-feed
0.6-0.8	10 ± 6	–	0.0 ± 0.1
0.8-1.0	120 ± 13	–	4.0 ± 0.5
1.0-1.2	27 ± 8	–	2.8 ± 1.0
1.2-1.4	70 ± 15	–	9.2 ± 3.2
1.4-1.6	77 ± 14	–	7.2 ± 4.4
1.6-1.8	49 ± 16	–	5.0 ± 2.9
1.8-2.0	53 ± 14	12 ± 7	7.3 ± 4.1
2.0-2.2	39 ± 17	16 ± 12	-2.0 ± 6.2
2.2-2.4	41 ± 16	30 ± 15	6.7 ± 2.2

Table 1: The data, $B\overline{B}$ and cross–feed yields for all final states in the nine M_{Had} bins with their statistical errors.

5 Signal Efficiency

The signal efficiency is determined from Monte Carlo samples using the yield for true signal events after cross-feed has been removed. In the first two M_{Had} bins, 0.6-1.0 GeV/c^2, the signal is modeled by the four exclusive $K^*\gamma$ modes. In the range 1.0–2.4 GeV/c^2, we use the inclusive $X_s\gamma$ model of Kagan and Neubert with $m_b = 4.65$ GeV/c^2. This inclusive model uses non-resonant JETSET [12] fragmentation of the X_S to produce the hadronic final states. Changing the modeling of the 1.0-1.2 GeV/c^2 bin to $K^*\gamma$, and varying the parameters of the inclusive model form part of our systematic studies.

The overall efficiency in each M_{Had} bin is an average over the individual final states, weighted by the fractional contribution of that final state to the total in that M_{Had} bin. These efficiencies have to be corrected by $\approx 10\%$ for the differences between data and Monte Carlo detection efficiencies for π^+, K^+, π^0, γ and K_S. There are significant differences between the efficiencies for the individual final states and a strong dependence of the overall efficiency on M_{Had}. To illustrate this, the

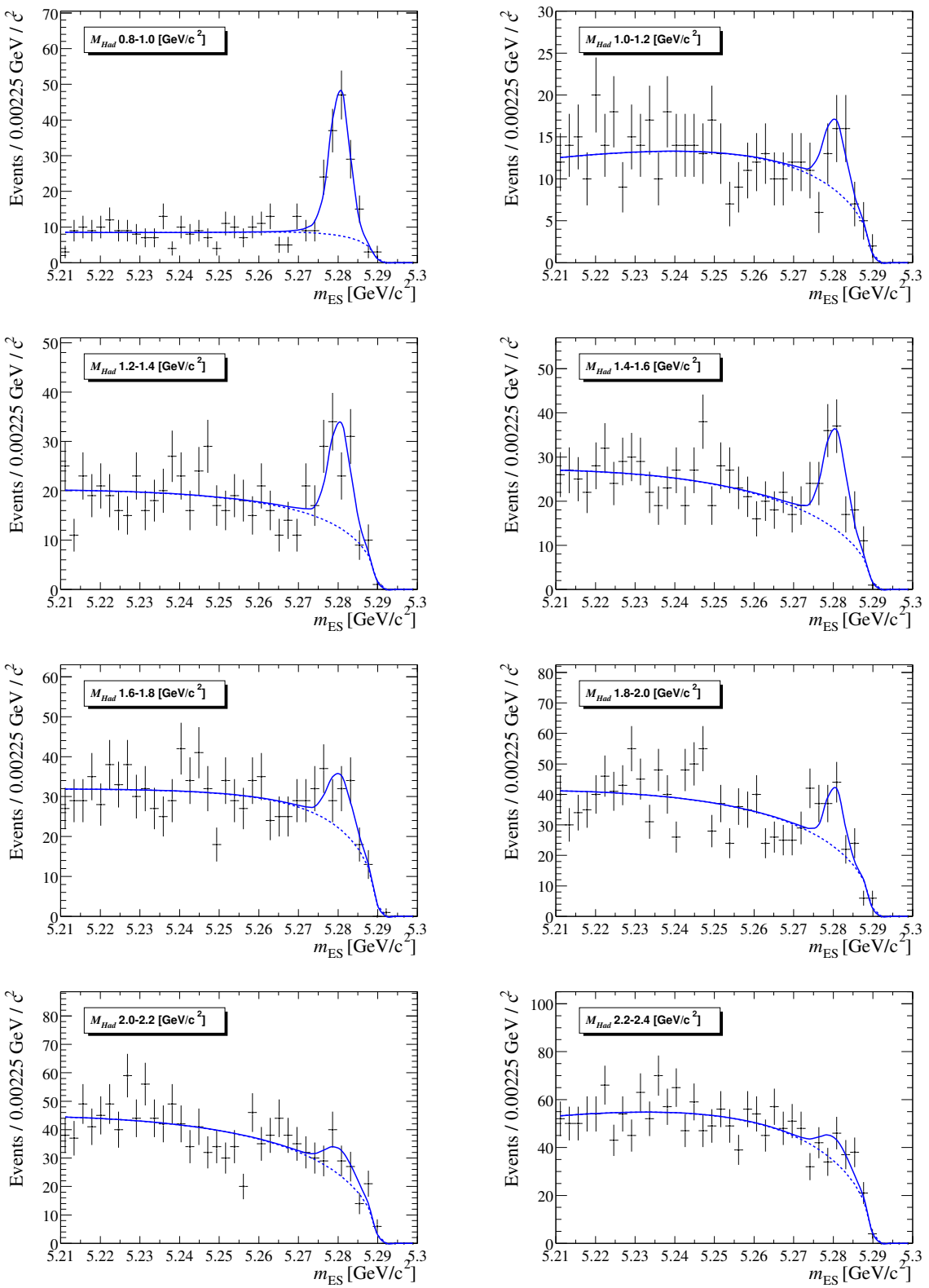

Figure 2: The fits to the data in bins of M_{Had} between 0.8 and 2.4 GeV/c^2.

efficiencies can be understood in terms of a $1/M_{Had}$ dependence of the efficiency for each final state, a 60% efficiency ratio between π^0 and π^+ final states, a 55% efficiency ratio between K_S and K^+ final states, and a 60% efficiency factor between 3 and 2–body, and between 4 and 3–body hadronic systems.

To check the fractions of each final state in the non-resonant Monte Carlo, we divide the sample above $M_{Had} = 1.0$ GeV/c^2 into three sets of final state categories: with and without a π^0, with and without a K_S, and 2, 3, or 4–body hadronic systems. A check of the K_S/K^+ samples shows that the data and Monte Carlo values agree, and the ratio K_S/K^+ is consistent with 0.5 as expected by isospin arguments. However, we find that the fraction of π^0 final states needs to be increased by a factor 1.5 and the fraction of 2–body final states decreased by a factor 0.4 in order to obtain a reasonable agreement between non-resonant Monte Carlo simulation and data. When these adjustments are applied to the fractions of final states generated by JETSET, they lead to a correction of $\approx 15\%$ in the overall efficiency. Table 2 presents the signal efficiencies after all corrections have been applied.

M_{Had} [GeV/c^2]	Efficiency
0.6-0.8	0.133 ± 0.009
0.8-1.0	0.094 ± 0.002
1.0-1.2	0.058 ± 0.004
1.2-1.4	0.045 ± 0.003
1.4-1.6	0.040 ± 0.002
1.6-1.8	0.034 ± 0.002
1.8-2.0	0.022 ± 0.002
2.0-2.2	0.022 ± 0.003
2.2-2.4	0.015 ± 0.003

Table 2: The corrected signal efficiencies in bins of M_{Had} with their statistical errors.

6 Branching Fractions

Partial branching fractions ($\Delta\mathcal{B}$) are calculated for each M_{Had} bin for the sum of the twelve final states reconstructed in this analysis. The calculation uses the data and $B\overline{B}$ yields from Table 1 and the signal efficiencies from Table 2. The peaking cross–feed background has to be normalized to our measured inclusive branching fraction ($\mathcal{B}$). We take care of this dependence of the peaking cross–feed background by including effective terms that modify the signal efficiencies in each bin, and report the equivalent peaking cross–feed yields in Table 1. Figure 3 shows the data yields after subtraction of the peaking $B\overline{B}$ and cross–feed backgrounds (signal yields).

The inclusive branching fraction for $b \to s\gamma$ in each M_{Had} bin can be obtained from the partial branching fractions by taking into account the fraction, f, of final states that are considered in the analysis. The fs are taken from the generator level JETSET fragmentation of the inclusive $b \to s\gamma$ signal. Since there are discrepancies in the modeling of our twelve reconstructed final states as already noted above, we know that the values of f are not completely reliable. There are also uncertainties coming from other final states, e.g. with η and ϕ mesons, which have not been looked for and therefore cannot be compared with data.

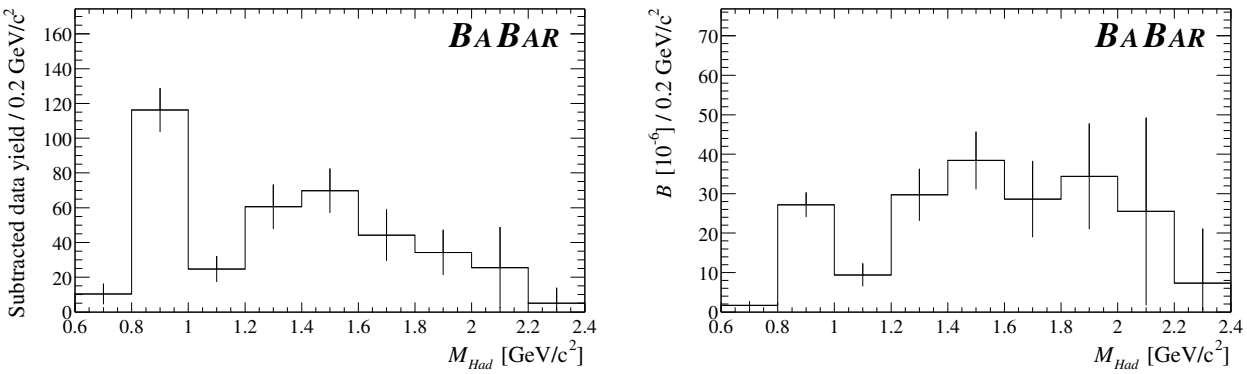

Figure 3: Signal yields (left plot) and weighted partial branching fractions (right plot), calculated with corrected efficiencies. Statistical errors only are shown.

We divide up the missing final states from our generator–level Monte Carlo into categories with a K_L (25%), more than one π^0 (4-18%), more than 4–body hadronic systems (0-14%), an η/η' (5-11%), a $s\bar{s}s$ system (0-7%), and "other"(0-4%), where the missing fractions increase from $M_{Had} = 1.0$ to $M_{Had} = 2.4$ GeV/c^2. The K_L fraction is known to be 25% from isospin and the measured K_S/K^+ ratio in data. For all the other fractions we allow a variation between 0.5 and 1.5 times the generator fraction, and add these variations in quadrature to give an overall systematic uncertainty on the missing fractions. Table 3 summarizes the partial branching fractions with their statistical errors, the fraction of studied final states with the corresponding errors, the resulting branching fractions with their statistical and systematic errors and the cumulative $b \to s\gamma$ branching fraction, with statistical and systematic errors, in bins of M_{Had}.

M_{Had} [GeV/c^2]	$\Delta\mathcal{B}\cdot 10^{-6}$	f (%)	$\mathcal{B}\cdot 10^{-6}$	Cumulative $\mathcal{B}\cdot 10^{-6}$
0.6-0.8	2 ± 1	75	$2.3 \pm 1.3 \pm 0.5$	$2.3 \pm 1.3 \pm 0.5$
0.8-1.0	27 ± 3	75	$36 \pm 4 \pm 5$	$39 \pm 4 \pm 5$
1.0-1.2	9 ± 3	66 ± 3	$14 \pm 4 \pm 4$	$53 \pm 6 \pm 7$
1.2-1.4	30 ± 7	63 ± 3	$47 \pm 10 \pm 9$	$100 \pm 12 \pm 14$
1.4-1.6	38 ± 7	55 ± 4	$70 \pm 13 \pm 13$	$170 \pm 18 \pm 25$
1.6-1.8	29 ± 10	45 ± 7	$64 \pm 22 \pm 15$	$233 \pm 28 \pm 36$
1.8-2.0	34 ± 13	35 ± 8	$98 \pm 38 \pm 30$	$332 \pm 48 \pm 61$
2.0-2.2	26 ± 24	27 ± 10	$95 \pm 88 \pm 43$	$426 \pm 100 \pm 98$
2.2-2.4	7 ± 14	22 ± 11	$33 \pm 63 \pm 62$	$460 \pm 118 \pm 134$

Table 3: The partial branching fractions ($\Delta\mathcal{B}$), the fraction of final states that are considered in the analysis (f), the total $b \to s\gamma$ branching fractions ($\mathcal{B}$) and the cumulative total $b \to s\gamma$ $\mathcal{B}$ in bins of M_{Had}. Statistical errors are shown for the $\Delta\mathcal{B}$s, and systematic uncertainties for the fs. Both statistical and overall systematic errors are shown for the $\mathcal{B}$s.

The systematic errors will be described in Section 7. It can be seen that the branching fraction for $M_{Had} < 1.0$ GeV/c^2 agrees with the exclusive $K^*\gamma$ branching fraction of about $4 \cdot 10^{-5}$ [5], and that the integral for $M_{Had} > 2.0$ GeV/c^2 is higher than previous measurements of the inclusive $b \to s\gamma$ branching fraction [13, 14], although with large uncertainties. Note that these results are

essentially independent of the modeling of the $b \to s\gamma$ spectrum.

Figure 4 shows the branching fractions as a function of M_{Had}. The same results are shown as a function of E_γ in Figure 5.

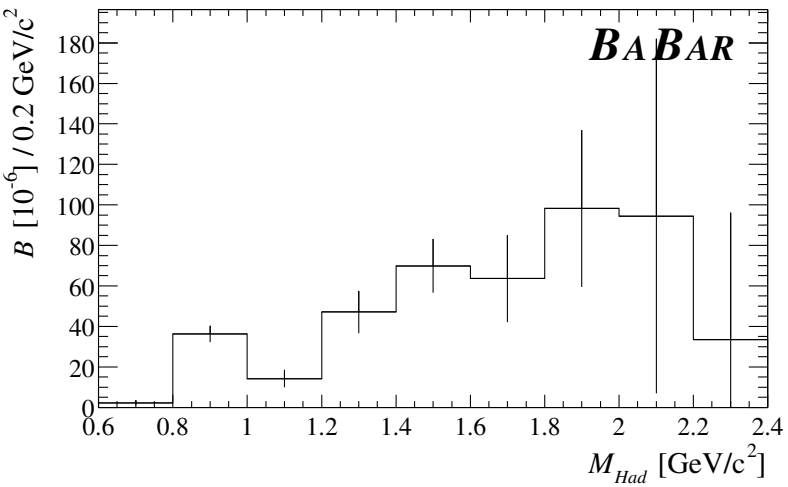

Figure 4: Branching fraction as a function of M_{Had}. The errors are purely statistical.

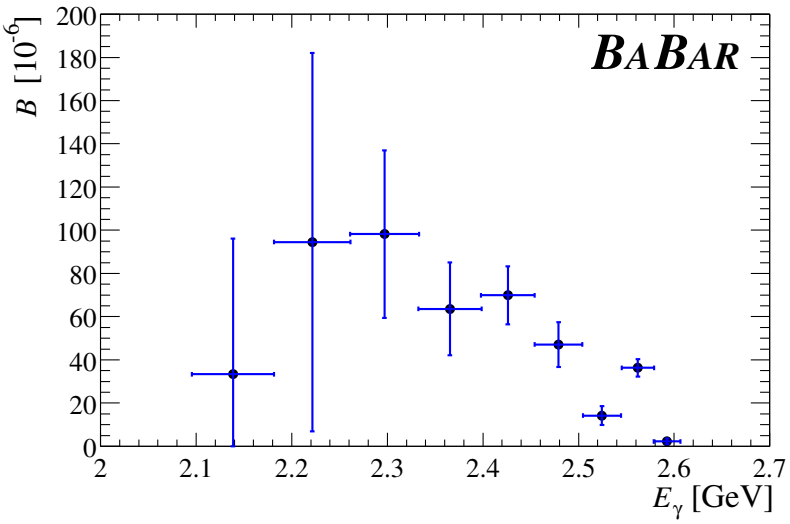

Figure 5: Branching fraction as a function of E_γ. The errors are purely statistical.

7 Systematic Errors

The first category of systematic errors (*general systematic*) are those which do not depend on the hadronic final state. The systematic error on the detection of the high–energy photon is 3.7%, and the systematic error on the total number of B mesons in our data sample is 1.6%. There is also a systematic uncertainty of 1% coming from the use of the $\cos\theta_{T*}$ and Fisher Discriminant requirements to suppress continuum backgrounds. These errors give a total contribution of 4.2% independent of the hadronic mass bin.

A second category of errors are due to the fitting procedure and signal definition (*fit systematic*). These errors are evaluated by varying the fixed parameters used in the fits, and by varying the fit procedures. The width of the signal Crystal Ball function is varied by ± 0.2 MeV/c^2 for both signal and peaking backgrounds. This introduces a systematic uncertainty of 5% on the signal yield. Varying the Crystal Ball shape to reflect our understanding of the radiative tail introduces a further systematic uncertainty of 5%, and varying the peak position introduces a systematic uncertainty of 3%. The ARGUS shape parameters are varied within the ranges allowed by the Monte Carlo samples. They give a contribution to the systematic uncertainty of 10%, which is limited by the Monte Carlo statistics. We also include a systematic error of 20% on the peaking $B\overline{B}$ yield in the region M_{Had}= 1.8-2.4 GeV/c^2 due to the method of fitting the $B\overline{B}$ yield, and to uncertainties in the content of the generic $B\overline{B}$ Monte Carlo simulation. This translates into a 10% systematic error in the last three M_{Had} bins.

Next we consider errors in the detection efficiencies for the hadronic final states (*efficiency systematic*). We assign systematic errors based on the uncertainties in the corrections to the efficiencies that we have applied. The uncertainties coming from the single particle detection differences between data and Monte Carlo are between 4.0 and 4.6% as a function of M_{Had}, and the fragmentation differences give uncertainties between 2.1 and 6.3%.

A final category of errors is due to the generator and modeling we use (*generator systematic*). The errors due to the missing final states not considered in the analysis were discussed in the previous section and shown in Table 3. Also, we consider contributions due to changing the modeling of the bin 1.0-1.2 GeV/c^2 to $K^*\gamma$ and varying the parameters of the inclusive model in our signal Monte Carlo.

The contributions to the systematic errors coming from all sources are summarized in Table 4.

M_{Had} [GeV/c^2]	*general systematic* (%)	*fit systematic* (%)	*efficiency systematic* (%)	*generator systematic* (%)	total systematic (%)
0.6-0.8	4.2	17	4.0	–	18
0.8-1.0	4.2	6	4.0	–	8
1.0-1.2	4.2	24	5.1	15	29
1.2-1.4	4.2	12	7.7	11	18
1.4-1.6	4.2	13	5.5	12	19
1.6-1.8	4.2	12	7.2	19	24
1.8-2.0	4.2	17	5.1	25	31
2.0-2.2	4.2	23	6.4	38	45
2.2-2.4	4.2	177	5.1	51	184

Table 4: All contributions to the systematic error are shown together with the total sum in quadrature as a function of the hadronic mass interval.

8 Fits to the Spectrum

So far our results have had no significant dependence on the $b \to s\gamma$ model. We now fit the hadronic mass spectrum with the shape predicted by the Kagan and Neubert model [4]. This extrapolates from the measured range of M_{Had} to give the inclusive branching fraction for $b \to s\gamma$.

In the fits we vary the parameters m_b and λ_1, the transition point between the K^* and non-resonant contributions, and the total normalization, which corresponds to our integrated branching fraction. In the plane λ_1 and m_b, Figure 6 shows the value of the χ^2, having fit the transition point (resulting around 1.1 GeV/c^2) and the normalization for each point. There is a strong correlation between these parameters, which is expected in this model, and a shallow minimum at $m_b = 4.65$ GeV/c^2 and $\lambda_1 = -0.48$ [GeV/c^2]^2. Figure 7(a) shows the correlation curve between λ_1 and m_b along which we have the minimum value of χ^2, and Figure 7(b) shows the values of χ^2 as a function of m_b. Figure 7(c) shows the inclusive branching fraction and the branching fraction for $M_{Had} < 2.4$ GeV/c^2 as a function of m_b, where the result for the minimum value of m_b found in the free fit is marked with a line. Since our spectrum contains a K^* peak with a known branching fraction of about $4 \cdot 10^{-5}$, a reduction in m_b leads to an increase in the non-resonant component of the spectrum, and hence to a higher inclusive branching fraction. This increase can be seen both in the branching fraction restricted to the measured range, and in the extrapolation over all M_{Had}.

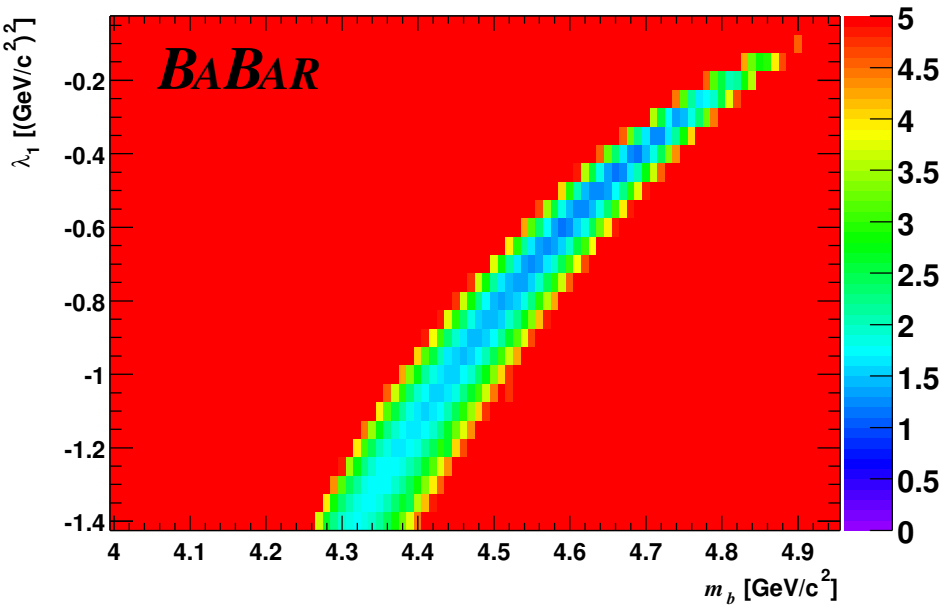

Figure 6: Minimum χ^2 value in the plane of λ_1, m_b. Values of the χ^2 larger than 5 are set to 5. Note the very strong correlation between λ_1 and m_b.

The free fit to the model parameters only allows us to set an upper bound on m_b, since the χ^2 rises rather slowly on the other side of the minimum. We obtain a lower bound on m_b by measuring the first moment of the E_γ distribution, $< E_\gamma >$, and then extracting $\overline{\Lambda}(\alpha_s^2, 1/M_B^3)$ using HQET calculations [15, 16] with the coefficients relevant for our minimum value of $E_\gamma = 2.094$ GeV [17]. Then, we truncate the HQET expressions to order $O(\alpha_s, 1/M_B^2)$ and recompute $m_b = M_B - \overline{\Lambda}(\alpha_s, 1/M_B^2)$ to obtain the parameter required in the Kagan and Neubert model. There are significant theoretical uncertainties associated with this method coming from varying the scale at which α_s is determined between $m_b/2$ and $2m_b$, from the truncation of higher–order terms, and from the dependence of $\bar{\Lambda}$ on the choice of the minimum E_γ [16].

The value of the first moment, $< E_\gamma > |_{E_\gamma > 2.094 \text{ GeV}}$, is:

$$< E_\gamma > |_{E_\gamma > 2.094 \text{ GeV}} = 2.35 \pm 0.04 \ (stat) \pm 0.04 \ (syst) \text{ GeV},$$

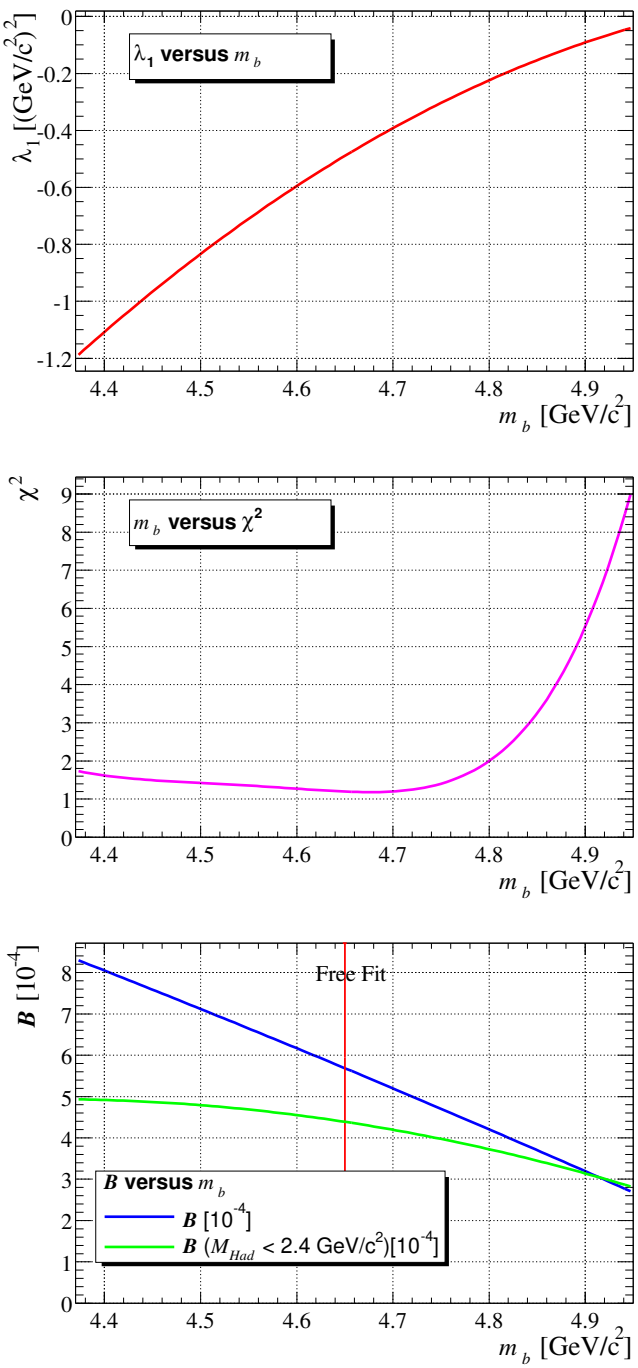

Figure 7: Results from a free fit to the M_{Had} spectrum. Plot (a) shows the correlation curve between λ_1 and m_b along which the χ^2 is minimized. Plot (b) shows the minimum χ^2 as a function of m_b. Plot (c) shows the inclusive $\mathcal{B}$ and the $\mathcal{B}$ for $M_{Had} < 2.4$ GeV/c^2 as a function of m_b.

which gives:

$$\overline{\Lambda} = 0.37 \pm 0.09\ (stat) \pm 0.07\ (syst) \pm 0.10\ (model)\ \ \mathrm{GeV}/c^2.$$

where the theoretical uncertainties have been included (*model*). With the truncation to first order in α_s, $\overline{\Lambda} = 0.49\ \ \mathrm{GeV}/c^2$, which gives:

$$m_b = 4.79 \pm 0.08\ (stat) \pm 0.10\ (syst) \pm 0.10\ (model)\ \ \mathrm{GeV}/c^2.$$

9 Final Results

We perform final fits to the hadronic mass spectrum with $m_b = 4.79 \pm 0.16\,\mathrm{GeV}/c^2$ taken from the first moment analysis. These fits give the inclusive branching fraction:

$$\mathcal{B}(b \to s\gamma) = 4.3 \pm 0.5\ (stat) \pm 0.8\ (syst) \pm 1.3\ (model) \cdot 10^{-4}$$

and a range for the parameter λ_1:

$$\lambda_1 = -0.24^{+0.03}_{-0.04}\ (stat) \pm 0.02\ (syst)^{+0.15}_{-0.21}\ (model)\ [\mathrm{GeV}/c^2]^2.$$

Figure 8 shows the superposition of the theoretical spectrum on the data distribution for the best fits with $m_b = 4.79\ \ \mathrm{GeV}/c^2$ and $m_b = 4.65\ \ \mathrm{GeV}/c^2$.

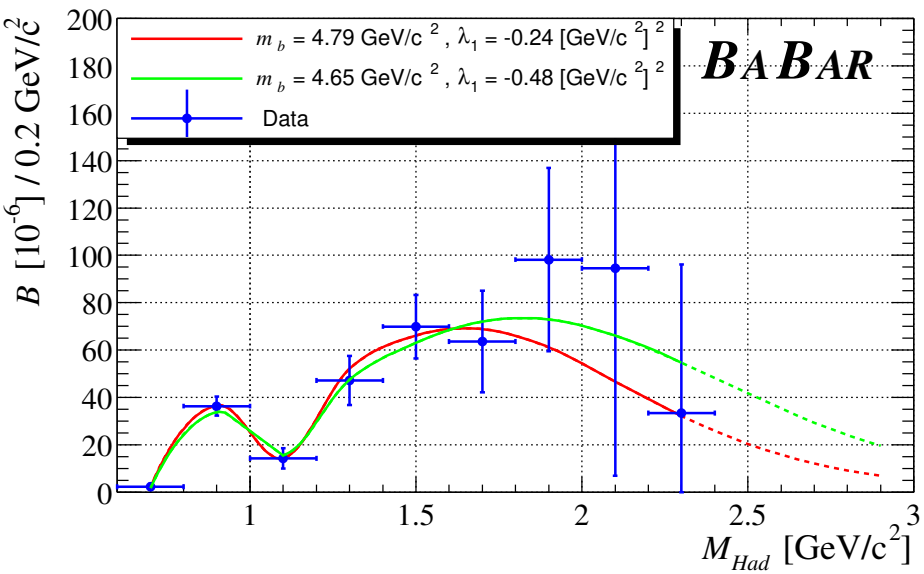

Figure 8: Superposition of the predicted spectrum for $m_b = 4.79\ \ \mathrm{GeV}/c^2$ and $m_b = 4.65\ \ \mathrm{GeV}/c^2$ on the observed hadronic mass spectrum.

Our values for $\overline{\Lambda}$, at $O(\alpha_s^2, 1/M_B^3)$, and λ_1, at $O(\alpha_s, 1/M_B^2)$, are consistent with other results [18], but our inclusive branching fraction is somewhat higher [13, 14]. Our error bars are still larger than the previous measurements, but they can be reduced significantly with the addition of more data. It is possible to reduce the systematic errors by improvements in the treatment of backgrounds, and by studying a larger number of final states to reduce the missing fraction errors. The model dependence will also be reduced by fitting the spectrum to determine the model parameters.

10 Acknowledgments

We would like to thank Alexander L. Kagan, Zoltan Ligeti and Mark B. Wise, for useful discussions and for having provided us with numbers and results from their works. We are grateful for the extraordinary contributions of our PEP-II colleagues in achieving the excellent luminosity and machine conditions that have made this work possible. The success of this project also relies critically on the expertise and dedication of the computing organizations that support *BABAR*. The collaborating institutions wish to thank SLAC for its support and the kind hospitality extended to them. This work is supported by the US Department of Energy and National Science Foundation, the Natural Sciences and Engineering Research Council (Canada), Institute of High Energy Physics (China), the Commissariat à l'Energie Atomique and Institut National de Physique Nucléaire et de Physique des Particules (France), the Bundesministerium für Bildung und Forschung and Deutsche Forschungsgemeinschaft (Germany), the Istituto Nazionale di Fisica Nucleare (Italy), the Research Council of Norway, the Ministry of Science and Technology of the Russian Federation, and the Particle Physics and Astronomy Research Council (United Kingdom). Individuals have received support from the A. P. Sloan Foundation, the Research Corporation, and the Alexander von Humboldt Foundation.

References

[1] K.G. Chetyrkin, M. Misiak, M. Munz, Phys. Lett. B **400**, 206 (1997), Phys. Lett. B **425**, 414 (1998);
P. Gambino and M. Misiak, Nucl. Phys. B **611**, 338 (2001);
A.J. Buras, A. Czarnecki, M. Misiak, J. Urban, Nucl. Phys. B **631**, 219 (2002).

[2] J.L. Hewett and J.D. Wells, Phys. Rev. D **55**, 5549 (1997).

[3] The *BABAR* Collaboration, B. Aubert *et al.*, CONF-02/026, SLAC-PUB-9301.

[4] A.L. Kagan and M. Neubert, Euro. Phys. Jour C **7**, 5 (1999), and private communication.

[5] The *BABAR* Collaboration, B. Aubert *et al.*, Phys. Rev. Lett. **88**, 101805 (2002).

[6] M. Neubert and T. Becher, Phys. Lett. B **535**, 127 (2002);
U. Aglietti, M. Ciuchini, P. Gambino, CERN-TH-2002-069.

[7] The *BABAR* Collaboration, B. Aubert *et al.*, Nucl. Instrum. Methods. **A479**, 1 (2002).

[8] The GEANT4 Collaboration, CERN-IT-2002-003, submitted to Nucl. Instrum. Methods A.

[9] G.C. Fox and S. Wolfram, Phys. Rev. Lett. **41**, 1581 (1978).

[10] The ARGUS Collaboration, H. Albrecht *et al.*, Z. Phys. C **48**, 543 (1990).

[11] E.D. Bloom and C. Peck, Ann. Rev. Nucl. and Part. Sci. **33**, 143 (1983).

[12] 'PYTHIA 5.7 and JETSET 7.4: Physics and manual', by Torbjorn Sjostrand (Lund U.), CERN-TH-7112-93-REV.

[13] The CLEO Collaboration, S. Chen *et al.*, Phys. Rev. Lett. **87**, 251807 (2001).

[14] The BELLE Collaboration, K. Abe *et al.*, Phys. Lett. B **511**, 151 (2001).

[15] Z. Ligeti, M.E. Luke, A.V. Manohar, M.B. Wise, Phys. Rev. D **60**, 034019 (1999).

[16] C. Bauer, Phys. Rev. D **57**, 5611 (1998).

[17] Z. Ligeti and M.B. Wise, private communication.

[18] The CLEO Collaboration, S. Chen *et al.*, Phys. Rev. Lett. **87**, 251808 (2001).